Supporting Information

Controllable synthesis of multidimensional carboxylic acid-based NiFe MOFs as efficient electrocatalysts for oxygen evolution

Kaihang Yue,[a,b] Jianglin Liu,[a] Chenfeng Xia,[c] Ke Zhan, [a] Ping Wang,[b,*] Xianying Wang,[b,*]and Ya Yan,[b,*]

Bao Yu Xia [c, *]

[a] School of Materials Science & Engineering, University of Shanghai for Science and Technology, 516 Jungong Road, Shanghai 200093, China

[b] CAS Key Laboratory of Materials for Energy Conversion, Shanghai Institute of Ceramics, Chinese Academy of Sciences (SICCAS), Shanghai 200050, China

[c] Key Laboratory of Material Chemistry for Energy Conversion and Storage (Ministry of Education), Hubei Key Laboratory of Material Chemistry and Service Failure, Wuhan National Laboratory for Optoelectronics, School of Chemistry and Chemical Engineering, Huazhong University of Science and Technology (HUST) 1037 Luoyu Road, Wuhan, 430074, PR China

*Corresponding author: wangping@mail.sic.ac.cn (P. Wang), wangxianying@mail.sic.ac.cn (X. Wang), and yanya@mail.sic.ac.cn (Y. Yan), byxia@hust.edu.cn (B. Y. Xia)

Experimental details

Materials and Chemicals: Nickel(II) nitrate hexahydrate ($Ni(NO_3)_2 \cdot 6H_2O$), Iron (III) chloride hexahydrate ($FeCl_3 \cdot 6H_2O$), N, N-Dimethylformamide (DMF), N, N-Dimethylacetamide (DMA), terephthalic acid (BDC), 2,5-Dihydroxyterephthalic Acid (DOBDC), 2-Aminoterephthalic Acid (NH_2BDC), Ethanol and potassium hydroxide (KOH) were purchased from Adamas Reagent Co., Ltd. Nickel foam was obtained from CeTech Co., Ltd. IrO_2 were obtained from Afar Aesar. All chemicals were used as they were received from manufacturers. Millipore high-purity water (DI, 18MΩ) was used in this study.

Synthesis of 1D-NiFe-BDC: In a typical fabrication procedure, 0.5mmol $Ni(NO_3)_2 \cdot 6H_2O$ and $FeCl_3 \cdot 6H_2O$ were dissolved in 12mL DMA to form a clear brown-yellow solution. Then 0.2 mmol terephthalic acid was added to the solution, and after stirring for 0.5 hours, the uniform solution was transferred to a Teflon vessel (20 mL) in sequence with a piece of clean Ni foam. Before taking out the sample from the vessel, the vessel was placed in a 120℃ oven for 3 hours and rinsed with ethanol and deionized water several times, then dry the sample at 60℃ for 8 hours.

Synthesis of 2D-NiFe-BDC /3D-NiFe-BDC: The preparation method of 2D/3D-NiFe-BDC is similar to the 1D-NiFe-BDC, except for the adjustment of the solvent. For 2D-NiFe-BDC, change the DMA to the same volume of DMF, ethanol, and deionized water mixed solution（Volume ratio 10:1:1）; for 3D-NiFe-BDC, adjust the DMA to a single DMF.

Synthesis of 2D-NiFe-DOBDC /2D-NiFe-NH_2BDC: The preparation method of 2D-NiFe-DOBDC /2D-NiFe-NH_2BDC is similar to the 2D-NiFe-BDC, except for changing the terephthalic acid (BDC) to the same molar amount of 2,5-dihydroxyterephthalic acid (DOBDC) or 2-aminoterephthalic acid (NH_2BDC).

Synthesis of NiFe-BDC with different solvent ratios or metal salt ratio: All samples are guaranteed to be prepared with the same molar amount of metal salt or the same volume of solvent. For example, a 2:1:1 solvent ratio is to use 6ml DMF, 3ml ethanol, and 3ml water as the reaction solvent; a 3:1 metal ratio is to use a metal salt with a molar ratio of 3:1 as the metal node.

Materials characterization: The morphologies and structure of the synthesized were characterized with field-emission scanning electron microscopy (FE-SEM, Quanta FEG450), transmission electron microscopy (TEM, FEI, TECNAI F30; Hitachi-HF5000), X-ray diffractor (XRD, D8 DISCOVER). The surface structure of the samples was characterized by nitrogen adsorption-desorption measurements at 77 K using the Brunauer-Emmett-Teller (BET, Autosorb iQ) method. The Fourier transform infrared spectroscopy (FT-IR, JASCO FT/IR-460) was recorded in the range of 4000–400 cm^{-1} with the sample pelleted using IR grade KBr. The

Raman spectrum (LabRam HR,) of as-prepared samples was conducted with a 30 mW He/Ne laser at 532 nm laser. X-ray photoelectron spectroscopy (XPS, ESCALAB250Xi, Thermo) with a dual anode Mg Kα as the excitation source, All XPS spectra are calibrated with C 1s at 284.8 eV as the standard.

Electrochemical measurement: All electrochemical performance of the catalyst was performed on a GAMRY workstation at room temperature. The electrolyze cell of three electrodes was used for all experiments while using the catalysts on NF as the working electrode, the graphite rod electrode served as the counter electrode, and Ag/AgCl as the reference electrode. 1 M KOH was employed as the electrolyte solution. All potentials in this article are measured relative to Ag/AgCl, but they were relative to the reversible hydrogen electrode (RHE) and are determined by $U_{RHE} = U_{Ag/AgCl} + 0.197 + 0.059 \times pH$. Cycle voltammetry (CV) of the OER test was performed from 0 V to 1 V vs. Ag/AgCl at a scan rate of $2mVs^{-1}$, and the electrochemical impedance spectroscopy (EIS) were measured in the frequency range of 0.01 Hz to 100 kHz. In addition, tested the CV curve at different scanning speeds, which are employed to estimate the double-layer capacitances (Cdl) of the catalysts. The catalyst was tested with chronopotentiometry curves （i-T） at 100mA to evaluate the stability of the catalyst.

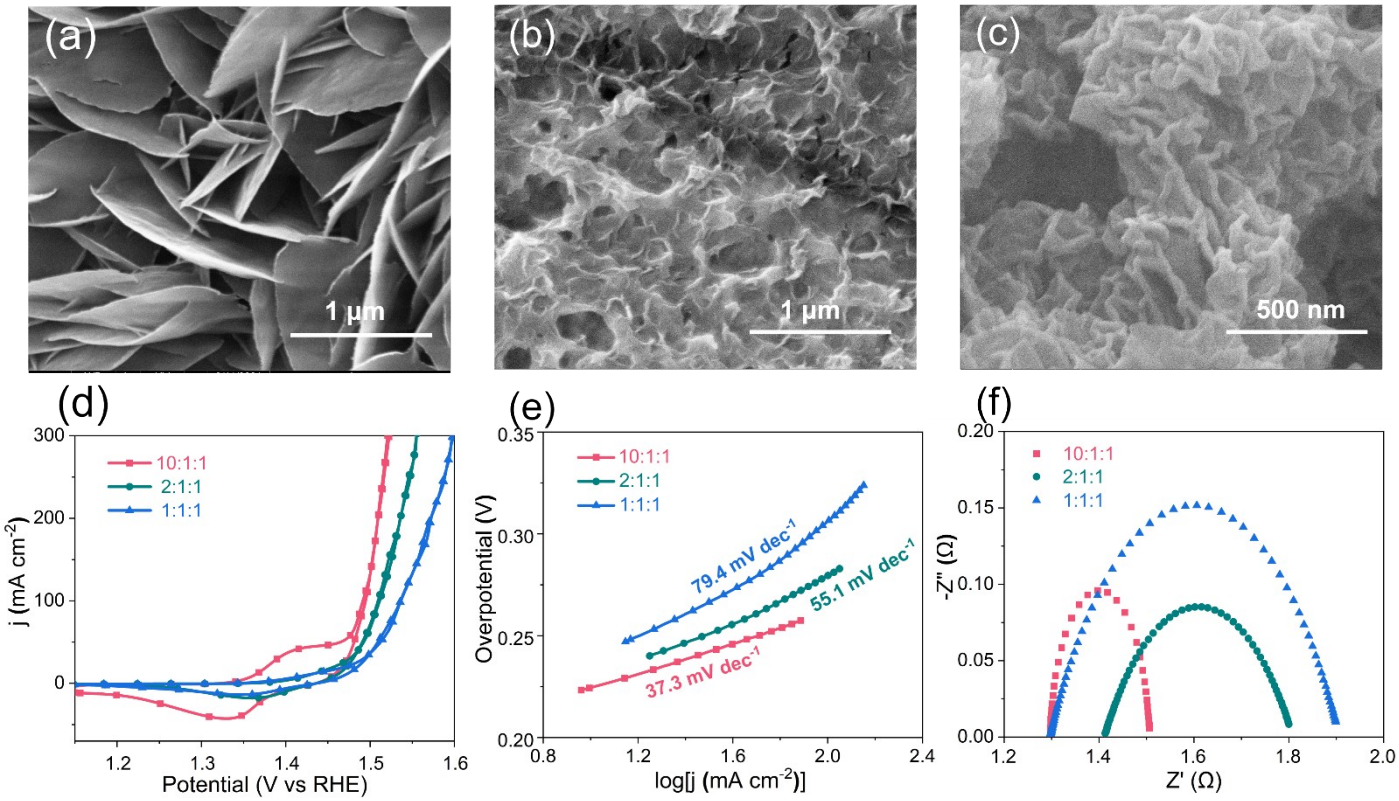

Figure S1 synthesized NiFe-BDC morphology obtained with different DMF: water: ethanol ratios (a)10:1:1, (b) 1:1:1, (c) 2:1:1**;** (d) cyclic voltammetry curves, (e) Tafel slopes, (f) Nyquist plots obtained by EIS of 2D-NiFe-BDC

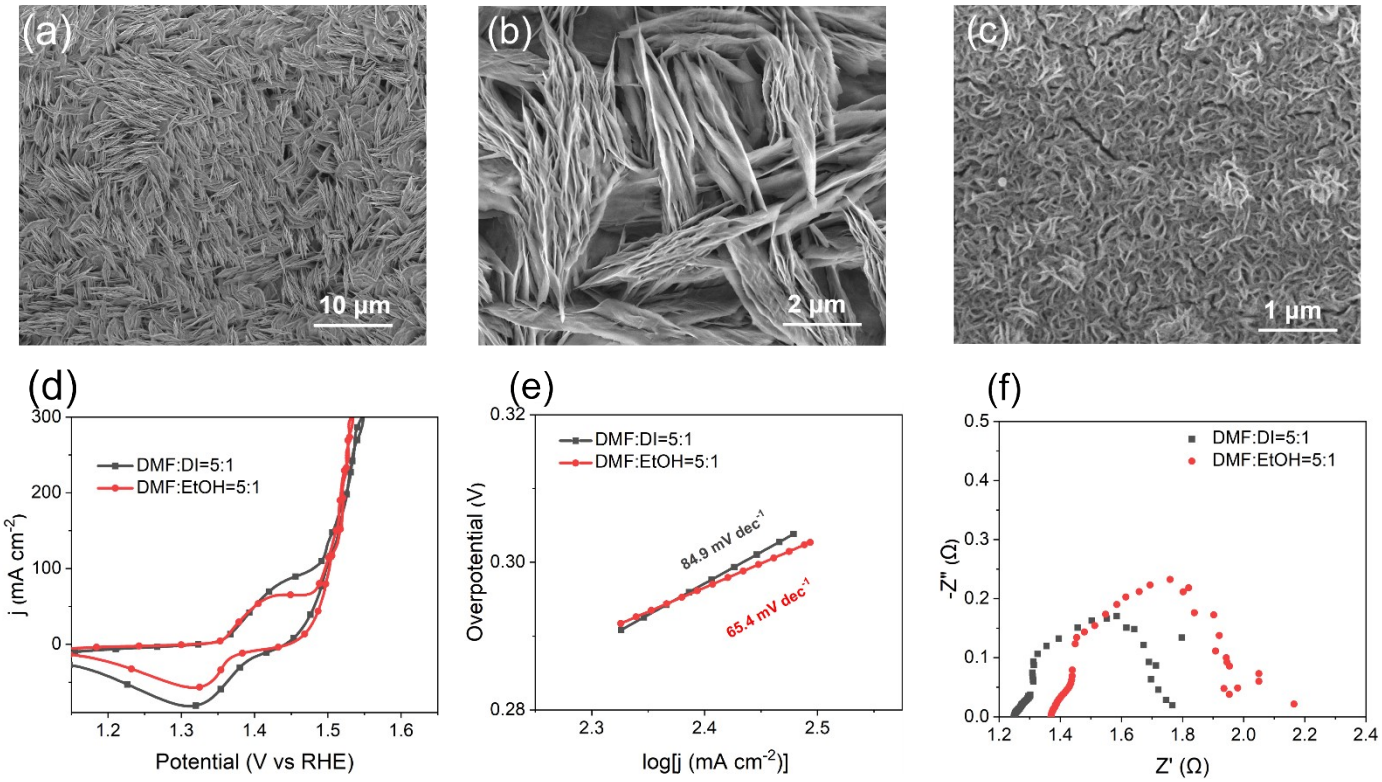

Figure S2 synthesized NiFe-BDC form obtained with mixed solvents (a-b) DMF: DI=5:1, (c) DMF: EtOH=5:1**;** (d) cyclic voltammetry curves, (e) Tafel slopes, (f) Nyquist plots obtained by EIS of NiFe-BDC

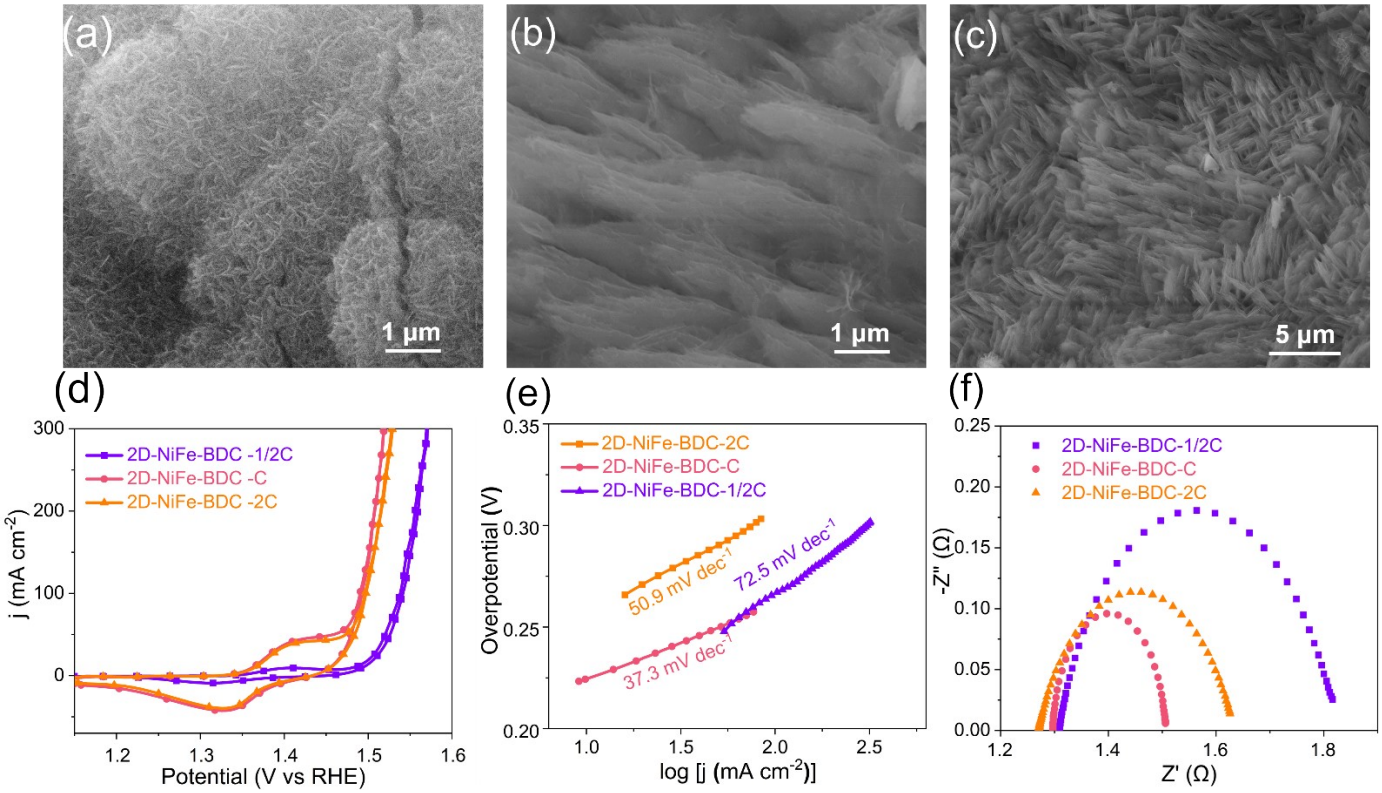

Figure S3 synthesized NiFe-BDC form obtained with different metal salt concentrations in a mixed solvent. (a) Half of the original concentration, (b-c)Twice the original concentration; (d) cyclic voltammetry curves, (e) Tafel slopes, (f) Nyquist plots obtained by EIS of NiFe-BDC

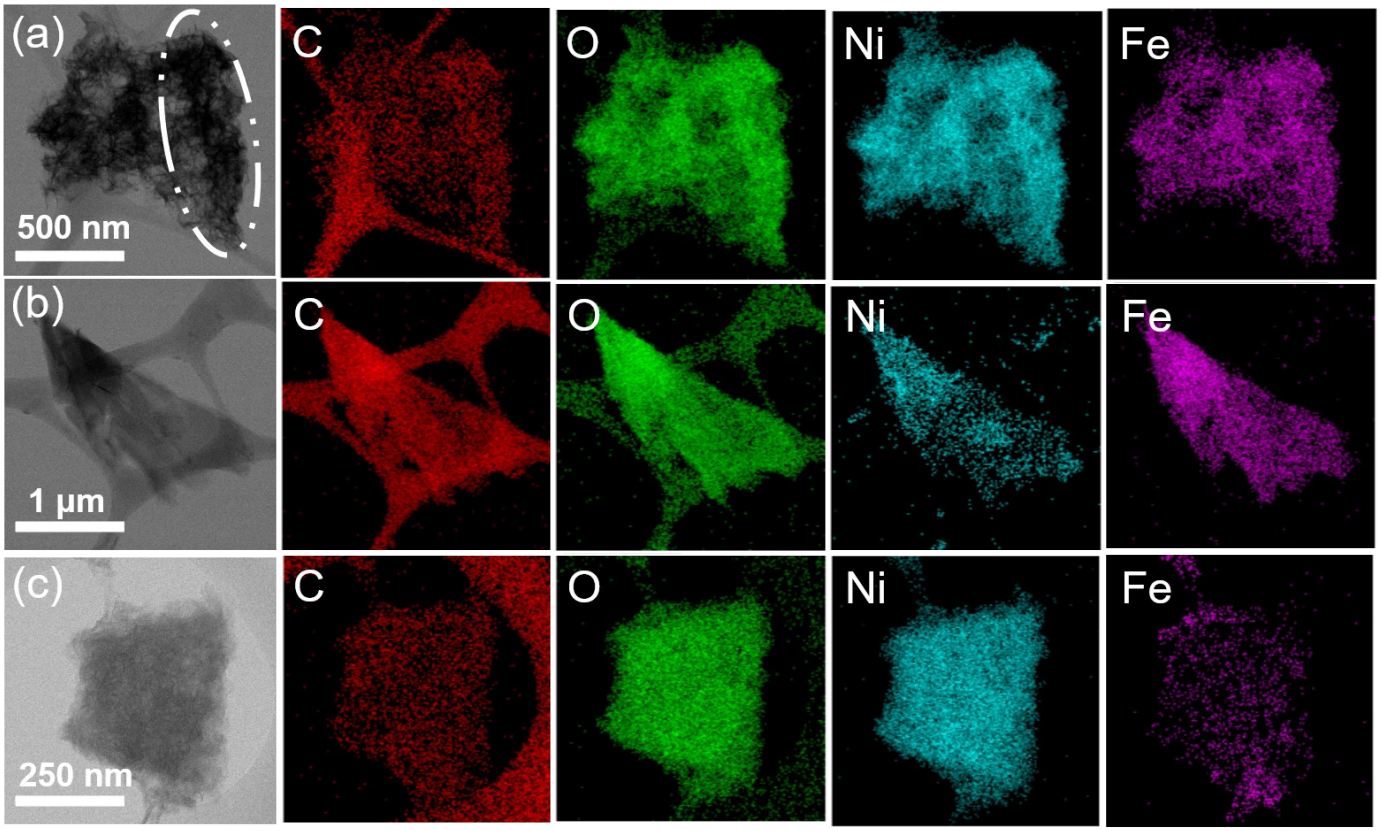

Figure S4 HAADF-STEM images and STEM-EDS mappings of (a)1D-NiFe-BDC, (b)2D-NiFe-BDC, (c)3D-NiFe-BDC.

(a)

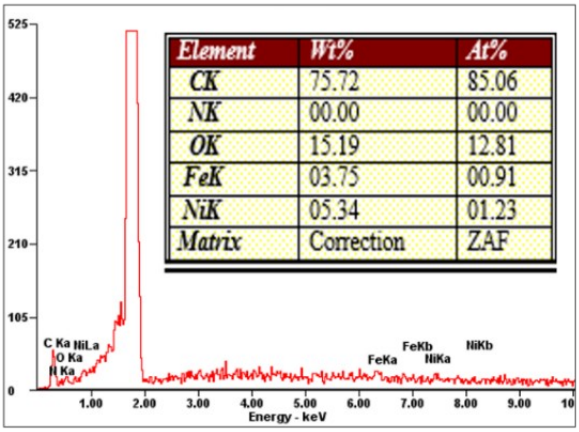

(b)

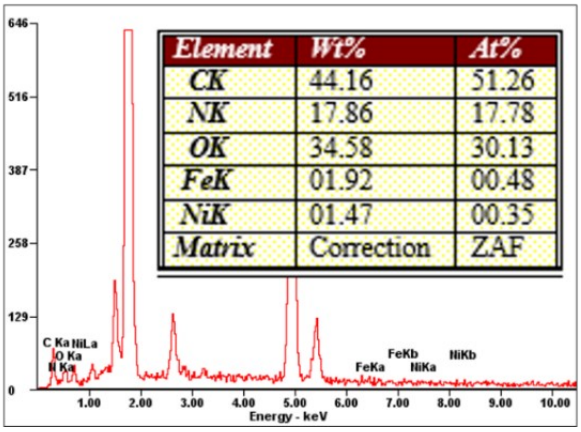

(c)

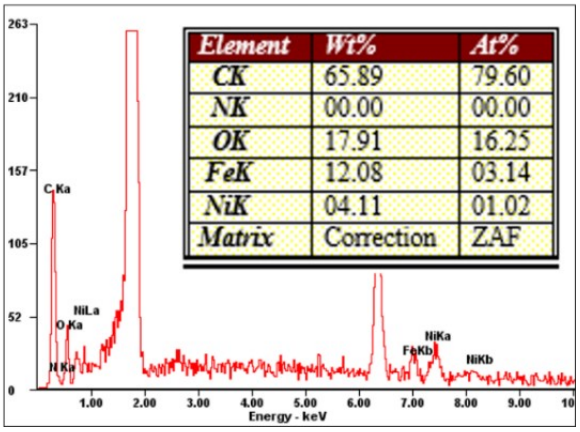

Figure S5 EDX spectrum of (a) 1D-NiFe-BDC, (b) 2D-NiFe-BDC (c) 3D-NiFe-BDC

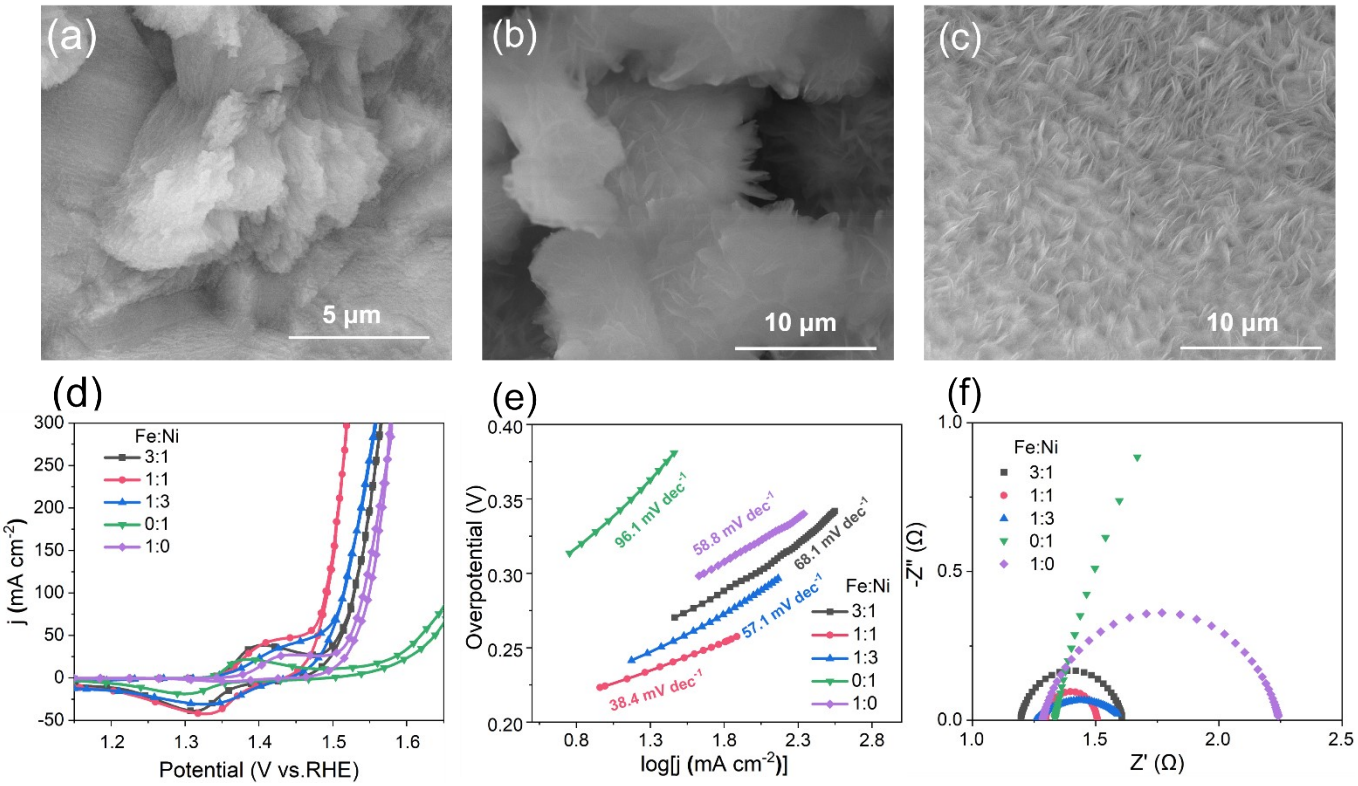

Figure S6 SEM images of BDC-MOF with different metal ratios (a) Fe: Ni=1:0 (b-c) Fe: Ni=0:1; (d) cyclic voltammetry curves, (e) Tafel slopes, (f) Nyquist plots obtained by EIS of BDC-MOF with different metal ratios.

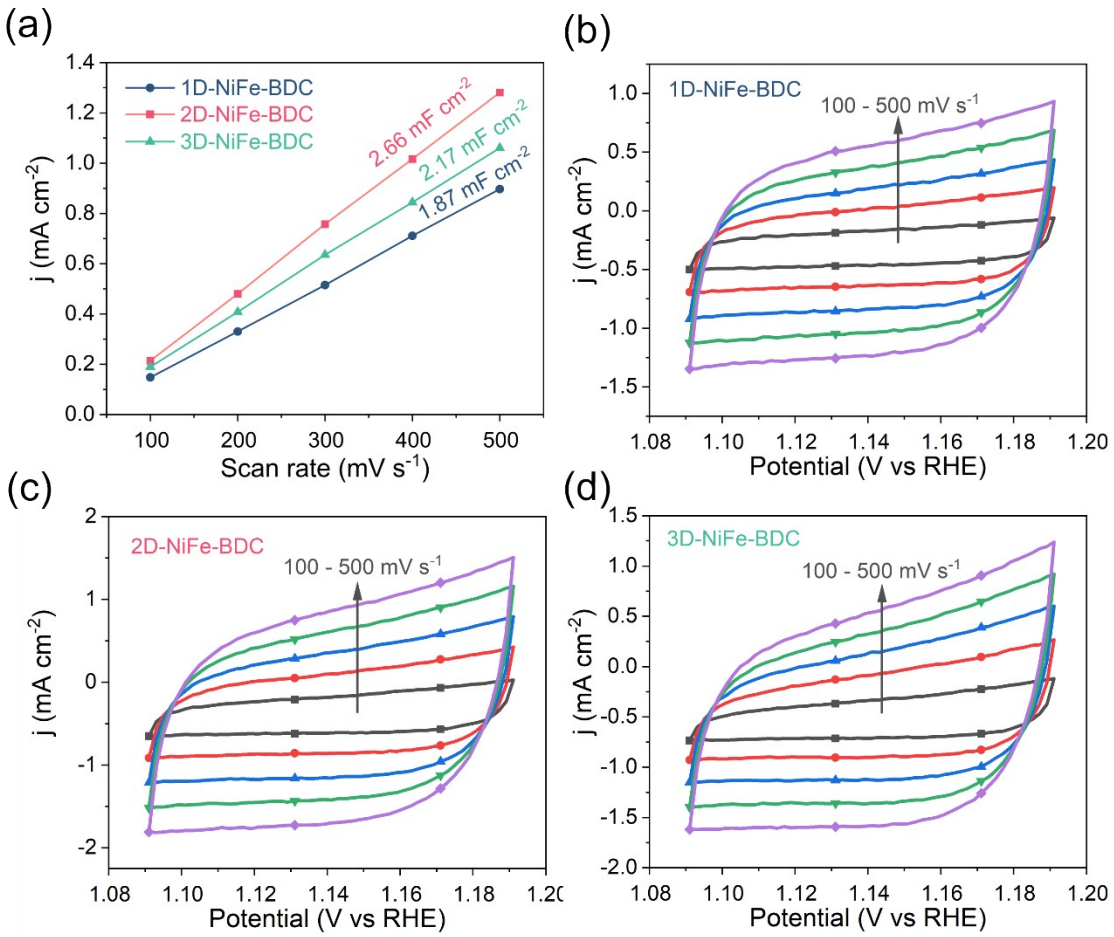

Figure S7 (a)Capacitive J versus scan rate for 1D, 2D, and 3D-NiFe-BDC, different scanning speeds CV curve of (b)1D-NiFe-BDC, (c)2D-NiFe-BDC, and (d)3D-NiFe-BDC.

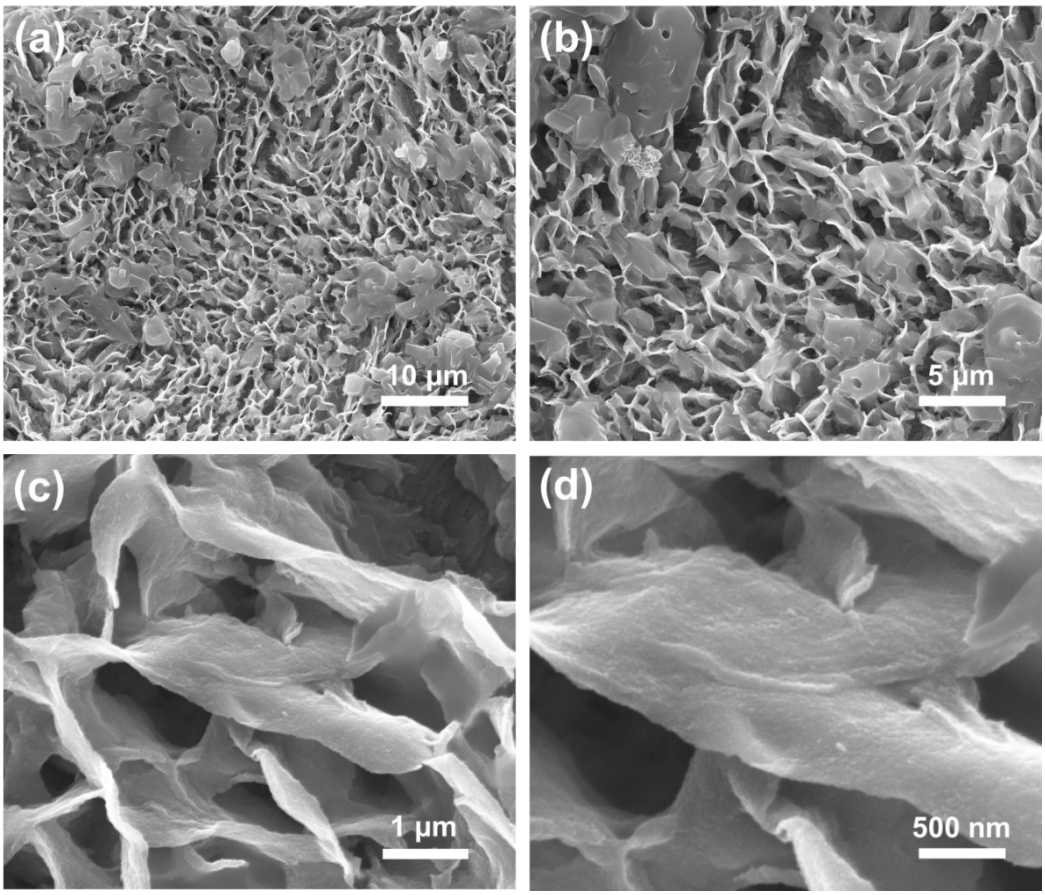

Figure S8 The SEM of 2D-NiFe-BDC after 70 h test.

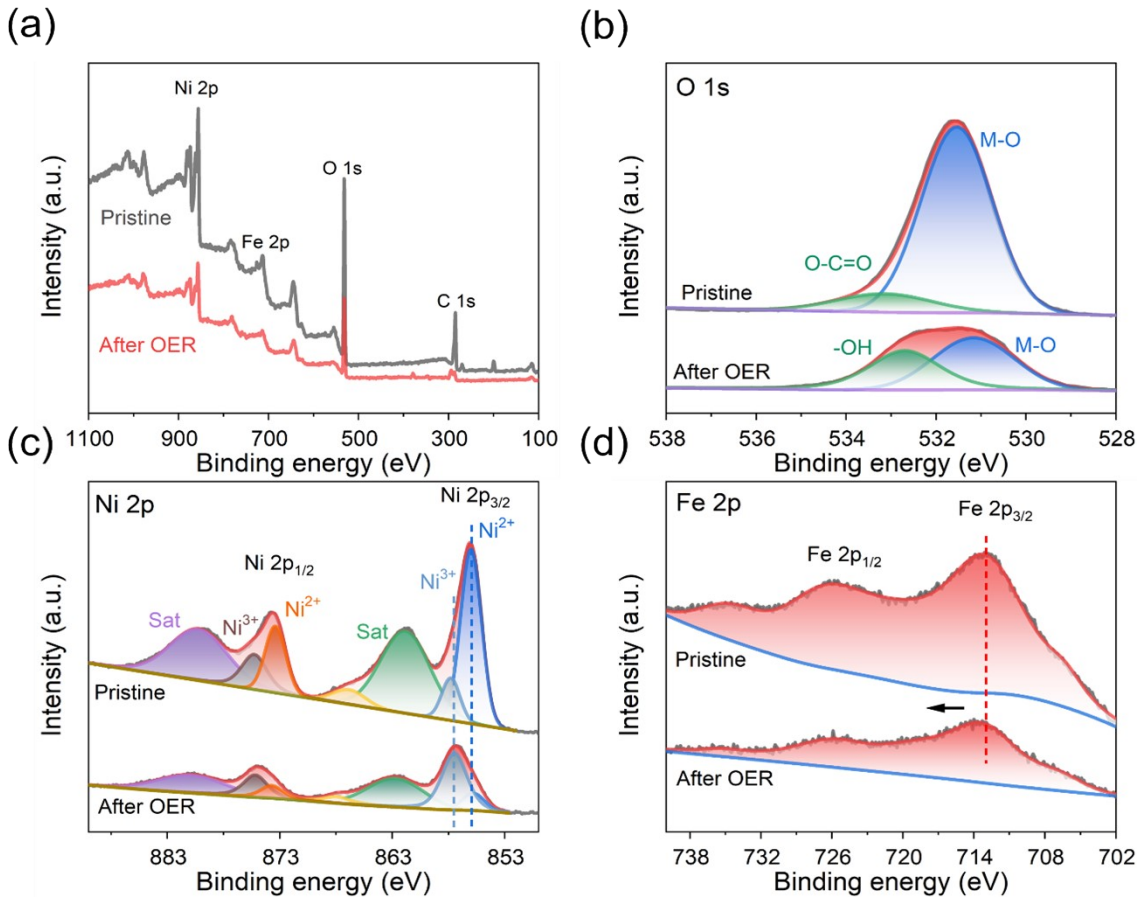

Figure S9 (a) XPS full survey spectra, (b) O 1s, (c) Ni 2p, (d) Fe 2p of pristine 2D-NiFe-BDC samples and post-test samples.

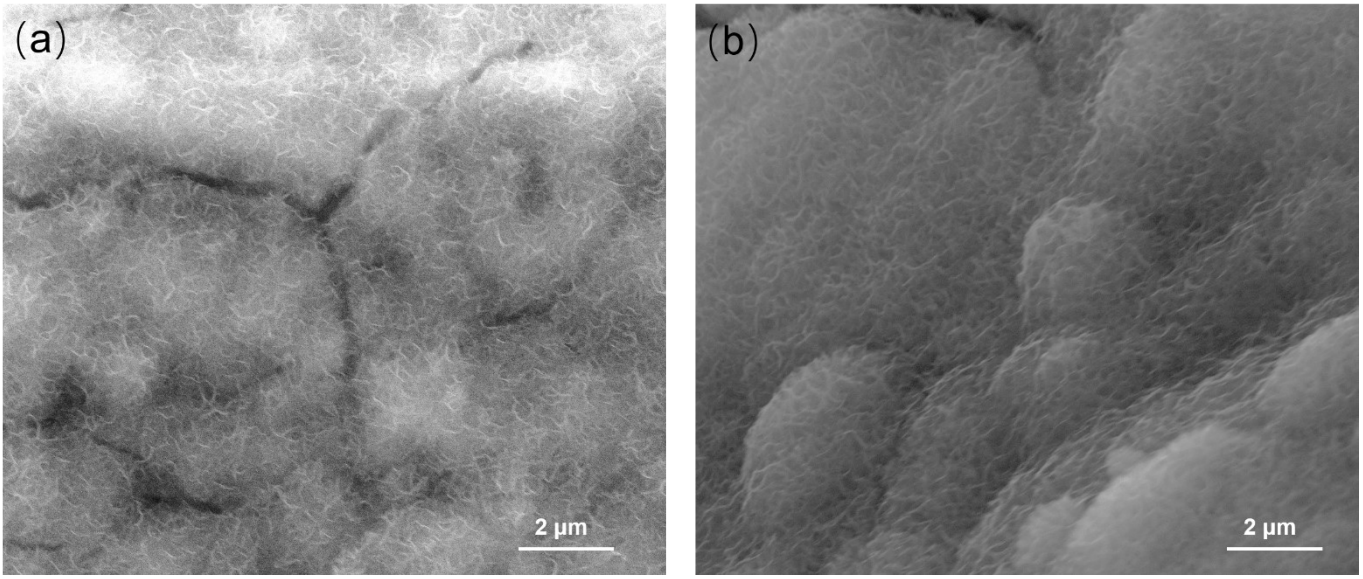

Figure S10 The SEM of (a) 2D-NiFe-DOBDC, (b) 2D-NiFe-NH_2BDC.

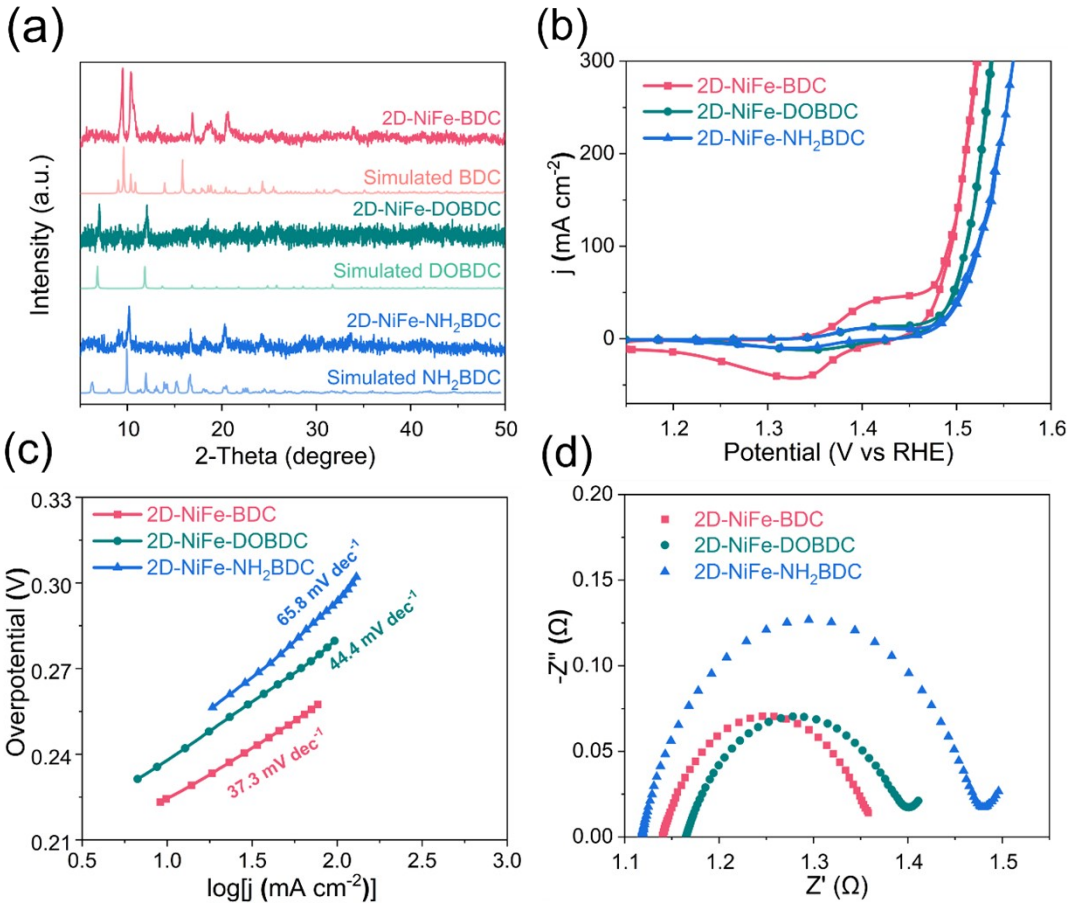

Figure S11 (a) XRD patterns, (b) cyclic voltammetry curves, (c) Tafel slopes, (d) Nyquist plots obtained by EIS of 2D-NiFe-BDC, 2D-NiFe-DOBDC, and 2D-NiFe-NH_2BDC

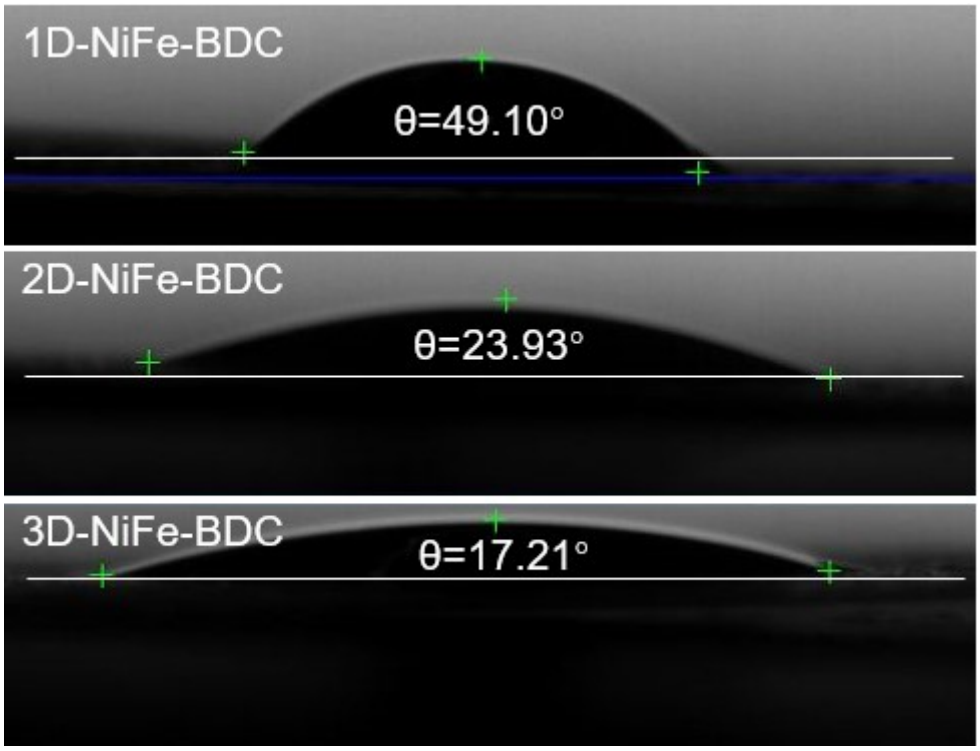

Figure S12 Contact angle measurements of the MOF samples (from bottom to top: 1D-NiFe-BDC, 2D-NiFe-BDC, and 3D-NiFe-BDC).

Table S1. Comparison of the OER activity with other carboxylic acid-based MOF catalysts previously reported.

Catalyst	Ligand	Overpotential (mV)	Tafel slope (mV dec^{-1})	Reference
2D-NiFe-BDC	BDC	223(η_{10}) 263(η_{100})	37.3	This work
$(Ni_2Co_1)_{0.925}Fe_{0.075}$-MOF	BDC	257(η_{10})	41.3	*Adv. Mater.* 2019, 31 (23), 1901139
Ni-MOF@Fe-MOF	BDC	265(η_{10})	82	*Adv. Funct. Mater.* 2018, *28* (26), 1801554
FN-2	BDC	316(η_{50})	56.7	*Small* 2019, *15* (45), 1903410
NiFe-NFF	BDC	253(η_{100})	38.9	*Adv. Funct. Mater.* 2018, *29* (6), 1807418
MIL-53(CoFe)/NF	BDC	262(η_{100})	69	*Nanoscale* 2020, *12* (1), 67-71
LIA-MIL-101(Fe)	BDC	225(η_{50})	60	*Adv. Funct. Mater.* 2021: 2102648
Ni 0.9 Fe 0.1 MOF	BDC	238(η_{10})	52	*Angew. Chem.* 133.21 (2021): 12204-12209
Ni 0.9 Fe 0.1 MOF				
2D-MOF-Fe/Co				
$Fe(OH)_3$@Co-MOF-74	DOBDC	292 (η_{10})	44	*ChemSusChem* 2019, *12* (20), 4623-4628
Fe-MOF-74 NAs@NF	DOBDC	207(η_{10})	41.1	*Chem. Commun.* 2019, *55* (75), 11307-11310

$NiCo/Fe_3O_4$/MOF-74	DOBDC	238(η_{10})	29	*J. Am. Chem. Soc.* 2018, *140* (45), 15336-15341
NH_2-BDC-$Fe_{0.5}Co_{0.5}$	NH_2BDC	410(η_{10})	101	*Chem. - Eur. J.* 2019, *25* (44), 10490-10498
NH_2-MIL-88B(Fe_2Ni)	NH_2BDC	240(η_{10})	143	*Adv. Energy Mater.* 2018, *8* (23), 1801065
NiFe-MOF/G	BTC	258(η_{10})	49	*Adv. Energy Mater.* 2021, 2003759
CoBDC-FC-NF	BTC	241(η_{10})	51	*Nat. Commun.* 2019, *10* (1), 5048
NiFe-BTC-GNPs	BTC	220(η_{10})	51	*Energy Environ. Sci.* 13.10 (2020): 3447-3458